AMERICAN SOCIETY FOR MICROBIOLOGY | Journal of Virology®

VIRUS-CELL INTERACTIONS

Deubiquitinating Enzyme USP21 Inhibits HIV-1 Replication by Downregulating Tat Expression

Wenying Gao,[a] Guangquan Li,[c] Simin Zhao,[b] Hong Wang,[a] Chen Huan,[a] Baisong Zheng,[a] Chunlai Jiang,[b] Wenyan Zhang[a]

[a]Institute of Virology and AIDS Research, Key Laboratory of Organ Regeneration and Transplantation of the Ministry of Education, The First Hospital of Jilin University, Changchun, China

[b]College of Life Science of Jilin University, Changchun, China

[c]Jilin Provincial Key Laboratory on Molecular and Chemical Genetics, The Second Hospital of Jilin University, Changchun, China

Wenying Gao and Guangquan Li contributed equally to this work. Author order was determined by seniority.

ABSTRACT Ubiquitination plays an important role in human immunodeficiency virus 1 (HIV-1) infection. HIV proteins such as Vif and Vpx mediate the degradation of the host proteins APOBEC3 and SAMHD1, respectively, through the proteasome pathway. However, whether deubiquitylating enzymes play an essential role in HIV-1 infection is largely unknown. Here, we demonstrate that the deubiquitinase USP21 potently inhibits HIV-1 production by indirectly downregulating the expression of HIV-1 transactivator of transcription (Tat), which is essential for transcriptional elongation in HIV-1. USP21 deubiquitylates Tat via its deubiquitinase activity, but a stronger ability to reduce Tat expression than a dominant-negative ubiquitin mutant (Ub-KO) showed that other mechanisms may contribute to USP21-mediated inhibition of Tat. Further investigation showed that USP21 downregulates cyclin T1 mRNA levels by increasing methylation of histone K9 in the promoter of cyclin T1, a subunit of the positive transcription elongation factor b (P-TEFb) that interacts with Tat and transactivation response element (TAR) and is required for transcription stimulation and Tat stability. Moreover, USP21 had no effect on the function of other HIV-1 accessory proteins, including Vif, Vpr, Vpx, and Vpu, indicating that USP21 was specific to Tat. These findings improve our understanding of USP21-mediated functional suppression of HIV-1 production.

IMPORTANCE Ubiquitination plays an essential role in viral infection. Deubiquitinating enzymes (DUBs) reverse ubiquitination by cleaving ubiquitins from target proteins, thereby affecting viral infection. The role of the members of the USP family, which comprises the largest subfamily of DUBs, is largely unknown in HIV-1 infection. Here, we screened a series of USP members and found that USP21 inhibits HIV-1 production by specifically targeting Tat but not the other HIV-1 accessory proteins. Further investigations revealed that USP21 reduces Tat expression in two ways. First, USP21 deubiquitinates polyubiquitinated Tat, causing Tat instability, and second, USP21 reduces the mRNA levels of cyclin T1 (CycT1), an important component of P-TEFb, that leads to Tat downregulation. Thus, in this study, we report a novel role of the deubiquitinase, USP21, in HIV-1 infection. USP21 represents a potentially useful target for the development of novel anti-HIV drugs.

KEYWORDS deubiquitinating enzyme, USP21, HIV-1 inhibition, Tat

The ubiquitin-proteasome system (UPS) is a major proteolytic system that controls protein degradation via posttranslational modification of proteins and plays an important role in almost all biological processes, including cancer progression, viral infection, innate immunity, viral restriction, and counterrestriction. It is well known that

Citation Gao W, Li G, Zhao S, Wang H, Huan C, Zheng B, Jiang C, Zhang W. 2021. Deubiquitinating enzyme USP21 inhibits HIV-1 replication by downregulating Tat expression. J Virol 95:e00460-21. https://doi.org/10.1128/JVI.00460-21.

Editor Frank Kirchhoff, Ulm University Medical Center

Address correspondence to Wenyan Zhang, zhangwenyan@jlu.edu.cn.

Received 17 March 2021
Accepted 30 March 2021
Accepted manuscript posted online 7 April 2021
Published 10 June 2021

UPS is often hijacked by human immunodeficiency virus 1 (HIV-1) to antagonize the host defensive factors during infection; for example, HIV-1 Vif degrades the apolipoprotein B mRNA-editing enzyme catalytic polypeptide-like 3G (APOBEC3G), HIV-2 Vpx degrades the Aicardi-Goutieres syndrome-related gene product sterile alpha motif (SAM) and HD domain containing protein-1 (SAMHD1), and HIV-1 Vpr degrades the helicase transcription factor (HLTF) through the proteasome pathway (1–5). In contrast, the host also uses UPS to degrade the invading viral proteins, thereby attenuating viral virulence or limiting viral infection (6–10).

Protein ubiquitination is reversed by a family of deubiquitylating enzymes (DUBs) that cleave peptide or isopeptide bonds between conjoined ubiquitin molecules or between ubiquitin and the modified proteins. DUBs can be subgrouped into seven subfamilies: ovarian tumor-related proteases (OTU), ubiquitin C-terminal hydrolases (UCH), ubiquitin-specific proteases (USP), Machado-Josephin domain-containing proteases (MJD), JAB1/MPN/MOV34 protease (JAMM) family, and two recently discovered MIU-containing novel DUBs, MINDY and zinc finger-containing ubiquitin peptidase 1 (ZUP1). DUBs have approximately 100 members in humans, and USP comprises the largest DUB subfamily (11, 12). In addition, viruses themselves encode DUBs to facilitate successful replication, such as the herpes simplex virus 1 (HSV-1)-encoded Ub-specific protease, UL36, Epstein-Barr virus-encoded BPLF1, and Middle East respiratory syndrome coronavirus-encoded Plpro (13–15). As the largest DUB subfamily, USPs regulate viral infection mainly via their deubiquitinase activity in several ways, including antiviral innate immune responses and virus-triggered apoptosis, among others. USP3 and USP21 deubiquitylate K63-linked polyubiquitin chains on RIG-I and act as negative regulators of vesicular stomatitis virus (VSV)-induced IRF3 phosphorylation and beta interferon (IFN-β) production, whereas USP4 significantly enhances RIG-I protein expression and RIG-I-triggered IFN-β through deubiquitination and stabilization of RIG-I (16–18). USP7 and BRCC36 stabilize HIV-1 Tat by promoting the deubiquitination of Tat, leading to enhanced viral production (19, 20). USP15 has been found to induce the degradation of HIV-1 Nef and structural protein Gag via ubiquitination and proteasomal pathways or both endosomal and proteasomal degradation pathways (21). A recent study reported that USP49 suppresses HIV-1 replication by deubiquitylating A3G, thereby inhibiting Vif-mediated A3G proteasomal degradation, resulting in the increased expression of the restrictive factor A3G (22). However, the role of DUB USPs in HIV-1 infection is largely unknown.

HIV-1 transactivator of transcription (Tat) is a critical regulator of transcriptional activation in HIV-1 that recruits the positive transcriptional elongation factor-b (P-TEF-b), composed of cyclin T1 (CycT1) and cyclin-dependent kinase 9 (CDK9), to the nascent transactivation response element (TAR) on the long terminal repeat (LTR) promoter, followed by the phosphorylation and activation of the paused RNAP II and viral gene expression (23). UPS is also essential for Tat stabilization and transcriptional activity. Nonproteolytic ubiquitination of Tat by Hdm2 is important for Tat-mediated transactivation, whereas ABIN1 inhibits Lys-63-linked ubiquitination of Tat via relocation of Hdm2 from the nucleus to the cytoplasm (24, 25). LncRNA NRON and curcumin mediate Tat ubiquitination and induce its degradation (9, 26). HIV-1 Rev reduces the levels of the ubiquitinated form of Tat and induces Tat degradation indirectly by downregulating NAD(P)H:quinine oxidoreductase 1 (NQO1) (27).

In this study, we screened the effect of some USP family members on HIV-1 infection and found that USP21 potently inhibits HIV-1 production by downregulating Tat expression. The deubiquitinase activity of USP21 is essential for Tat downregulation; however, in addition to deubiquitinating Tat ubiquitination, USP21 also decreases CycT1 mRNA levels through epigenetic modification, which is necessary for Tat stabilization (28). Hence, we show that USP21 is a novel and selective regulator of HIV-1 Tat. Our finding provides an important target for HIV-1 drug development and treatment.

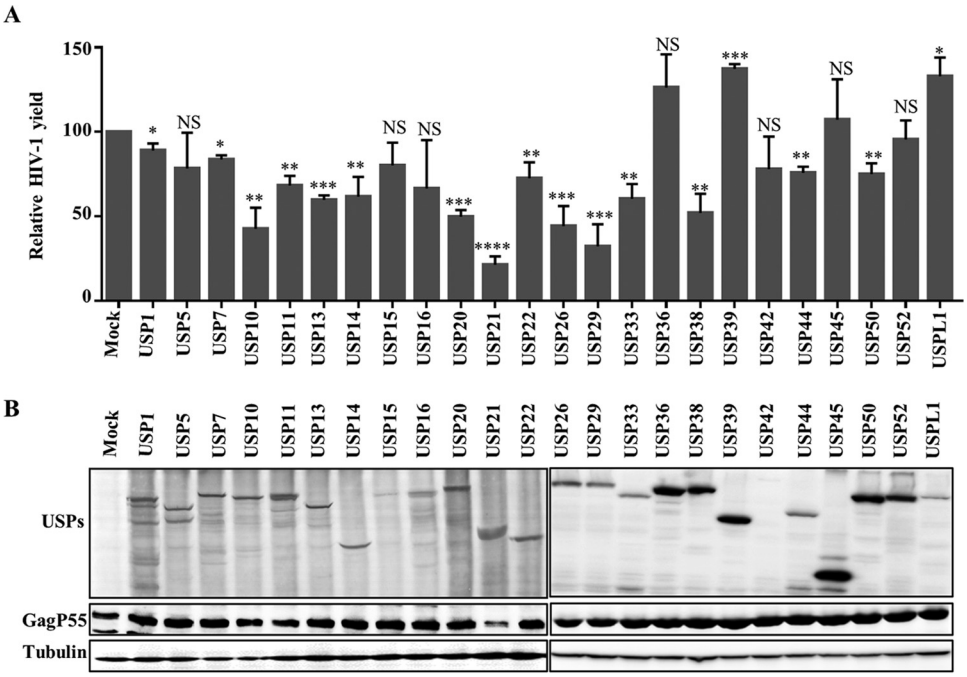

FIG 1 Screening of USP family members with anti-HIV-1 activity. The effect of overexpression of 24 deubiquitinase USPs on HIV-1 viral yield is shown. HIV-1 expression vector pNL4-3 and USP expression vectors with HA tag or control vector were cotransfected into HEK293T cells. (A) After 48 h, the viral supernatant was harvested and used to infect TZM-b cells. HIV-1 viral yield was assessed using TZM-bl indicator cells, with HIV-1 infectivity in the absence of USP set to 100%. (B) The cells were harvested and protein expression was analyzed by immunoblotting (IB) with anti-HA antibody targeting USP proteins and CAp24 antibody targeting HIV-1 viral proteins. Tubulin was used as a loading control. Statistical significance was analyzed using two-sided unpaired *t* tests (NS, not significant; *, $P < 0.05$; **, $P < 0.01$; ***, $P < 0.001$; ****, $P < 0.0001$).

RESULTS

USP21 potently inhibits HIV-1 production. Because of the essential role of the UPS in HIV-1 infection, we screened the effect of a few DUB USPs on HIV-1 replication. To determine whether the USPs inhibit HIV-1 replication, we purchased a series of USP family members from Addgene and examined their anti-HIV-1 ability. We transfected HEK293T cells with pNL4-3 expression vector plus the negative-control vector VR1012 or the indicated USP expression vector and then harvested cells 48 h later for immunoblotting and analysis of infectious HIV-1 production. We found that infectious HIV-1 production was greatly decreased in the presence of USP21 when TZM-bl cells were used as indicator cells for infection (Fig. 1A), whereas USP10, USP13, USP20, USP26, USP29, USP33, USP38, USP44, and USP50 moderately affected the HIV-1 yield. The other USP members showed no effect. The levels of USPs and Gagp55 were determined by immunoblot (IB) analysis (Fig. 1B). USP21 also obviously decreased intracellular Gagp55 expression. With increasing doses of USP21, the expression of Gagp55 and CAp24 in the cell lysate and viral supernatant, respectively, as well as the infectious HIV-1 yield, decreased in a dose-dependent manner (Fig. 2A and B), further confirming that USP21 suppresses HIV-1 production. In contrast, compared to a short hairpin RNA (shRNA) negative control (shRNA NC), stable knockdown of USP21 (sh-USP21) in HEK293T cells led to increased levels of Gagp55 in the cell lysate and CAp24 in the viral supernatant (Fig. 2C). Infectious HIV-1 production in the supernatant of USP21 shRNA cells increased by approximately 2-fold (Fig. 2D).

To further determine whether infectious HIV-1 production in target T cells was affected by USP21 over time, we constructed stable USP21 knockdown Jurkat cells using shRNA targeting USP21 and shRNA NC (Fig. 2E and F). Knockdown of USP21 induced an approximately 1.5-fold increase in the yield of infectious HIV-1 compared to shRNA NC in Jurkat cells on day 2, and this yield of infectious HIV-1 was maintained

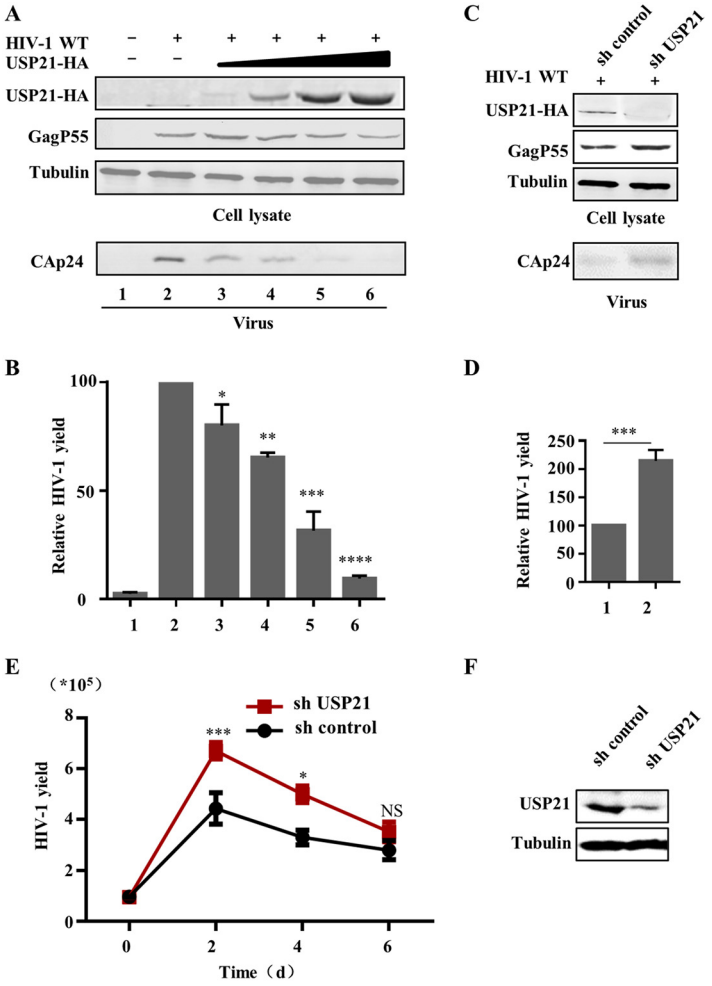

FIG 2 USP21 potently inhibits HIV-1 production in a dose-dependent manner. (A) Various amounts of USP21 expression vector (100, 200, 400, and 800 ng) or negative-control vector were transfected along with pNL4-3 viral expression vector into HEK293T cells. After 48 h, cells and the viral particles from the supernatants were harvested and analyzed by IB. (B) Infectious HIV-1 production was decreased with increasing USP21 expression, as detected using TZM-bl indicator cells. Infectious HIV-1 production in the absence of USP21 was set as 100%. (C and D) Knockdown of USP21 increased HIV-1 production. Stable pLKO.1- and sh-USP21-expressing cell lines constructed in HEK293T cells were transfected with HIV-1 expression vector for 48 h. (C) Cells and supernatants were harvested for IB analysis. HIV-1 yield was measured by detecting the luciferase activity following infection of TZM-bl cells with the supernatant for another 48 h. (D) The infectious HIV-1 production of shRNA NC was set as 100%. (E and F) USP21 inhibits HIV-1 production in T cells. (E) Knockdown of USP21 promoted infectious HIV-1 production in $CD4^+$ T cells. Stable sh-USP21-expressing cell lines were constructed with Jurkat cells, infected with HIV NL4-3 virus for 12 h, washed twice with PBS buffer, and cultured in fresh RPMI 1640 medium with 10% FBS. Cell supernatants were then harvested 0, 2, 4, and 6 days postinfection. Viral yield was assessed using TZM-bl indicator cells. (F) USP21 expression was analyzed by IB, and tubulin was used as a loading control. All data are presented as the means ± standard deviations (SD) from three independent experiments (*, $P < 0.05$; **, $P < 0.01$; ***, $P < 0.001$; ****, $P < 0.0001$).

until day 6 (Fig. 2E). USP21 knockdown in Jurkat cells was confirmed by IB analysis (Fig. 2F). Collectively, these data suggest that USP21 strongly inhibits HIV-1 production.

USP21 has no effect on the function of HIV auxiliary proteins (Vif, Vpx, Vpr, and Vpu). USP21 is a deubiquitinase that removes polyubiquitination from target proteins. HIV accessory proteins Vif, Vpx, and Vpr recruit host E3 ubiquitin ligase complexes to induce polyubiquitination of the host restriction factors A3G, SAMHD1, and HLTF (1, 2, 4, 5, 29), whereas Vpu is involved in BST-2 degradation through the proteasomal or lysosomal pathways (30). Therefore, we sought to determine whether USP21 causes deubiquitination of ubiquitinated A3G, SAMHD1, HLTF, or BST-2 to protect host

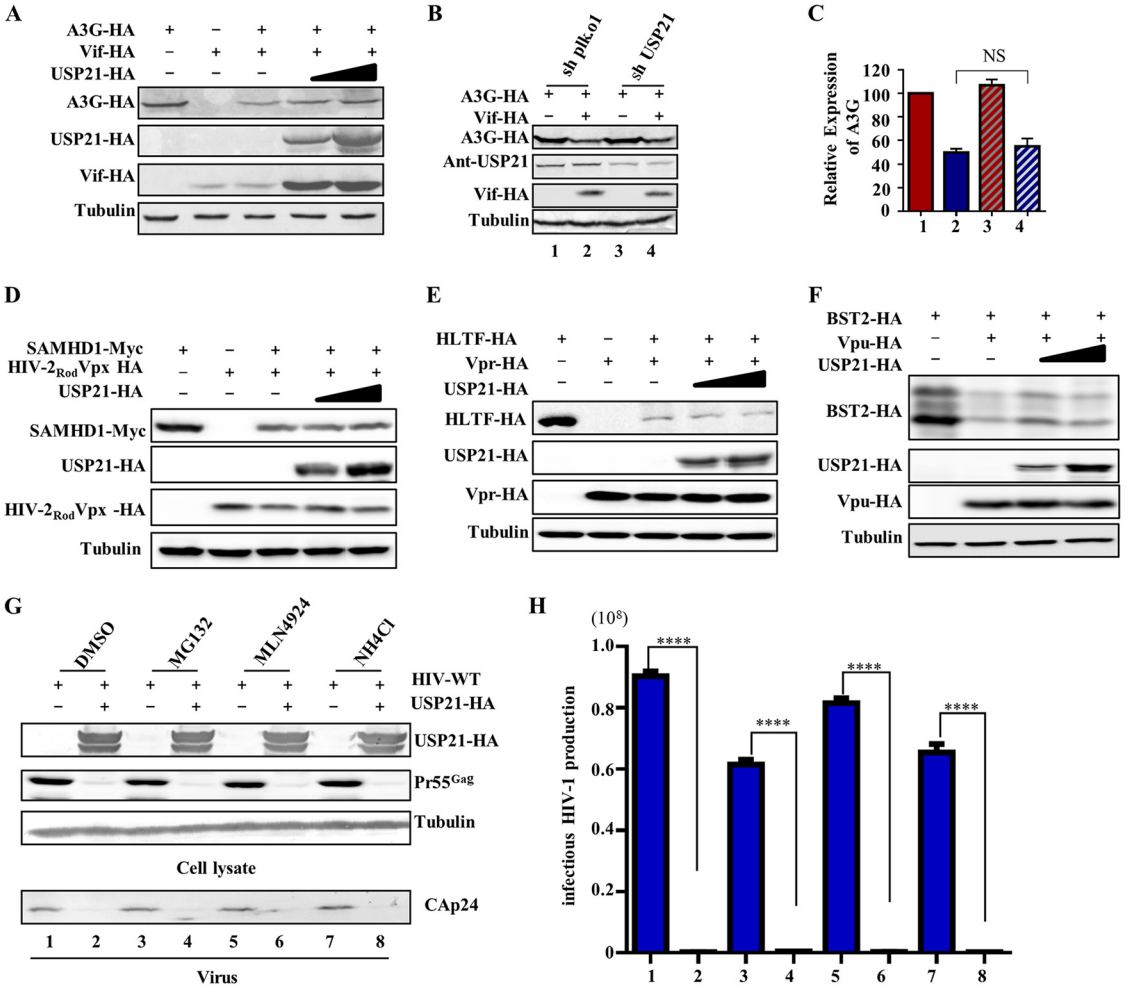

FIG 3 USP21 has no effect on the function of HIV-1 auxiliary proteins (Vif, Vpx, Vpr, and Vpu). (A) Overexpression of USP21 has no effect on Vif-mediated A3G degradation. HEK293T cells were transfected with expression vectors as indicated. Cell lysates were immunoblotted with the corresponding antibodies. (B and C) Knockdown of USP21 in HEK293T had no effect on the function of Vif. (B) Stable sh-USP21-expressing cells were transfected with expression vectors as indicated. Cell lysates were immunoblotted with the corresponding antibodies. (C) A3G expression was quantified using Image J software to calculate the values relative to that of tubulin. Overexpression of USP21 had no effect on Vpx-mediated SAMHD1 degradation (D), Vpr-mediated HLTF degradation (E), or Vpu-mediated degradation of BST2 (F). HEK293T cells were transfected with expression vectors as indicated. Cell lysates were immunoblotted with the corresponding antibodies. (G and H) USP21 reduced HIV-1 production independent of proteasome pathway. (G) HIV-1 was cotransfected along with VR1012 or USP21 into cells for 24 h, and the cells were treated with 10 μM MG132, 1 μM MLN4924, and 20 μM NH_4Cl for 12 h before harvest. The cell lysates were immunoblotted with the corresponding antibodies (G), and HIV-1 yield from cell supernatants was assessed using TZM-bl indicator cells (H). Statistical significance was analyzed using two-sided unpaired *t* tests (NS, not significant; *, $P < 0.05$; **, $P < 0.01$; ***, $P < 0.001$; ****, $P < 0.0001$).

factors from degradation and results in HIV inhibition. We first examined whether overexpression or knockdown of USP21 influences the degradation of A3G by Vif. The data showed that USP21 had no effect on Vif-mediated A3G degradation (Fig. 3A to C). We also observed that increasing the amount of USP21 had no effect on Vpx-mediated SAMHD1, Vpr-mediated HLTF, or Vpu-mediated BST-2 degradation (Fig. 3D to F), suggesting that USP21 inhibition on HIV-1 was not associated with functions of the HIV-1 auxiliary proteins. These data demonstrated that the USP21-mediated regulation of HIV-1 infectivity was not due to the removal of polyubiquitination from the host factors A3G, SAMHD1, HLTF, and BST-2 and promoted their expression. To examine whether USP21-mediated reduction in HIV-1 production was associated with proteasome or lysosome degradation pathways, HIV-1 wild type (WT), USP21, or the control vector VR1012 was cotransfected into HEK293T cells. After 24 h, different inhibitors were

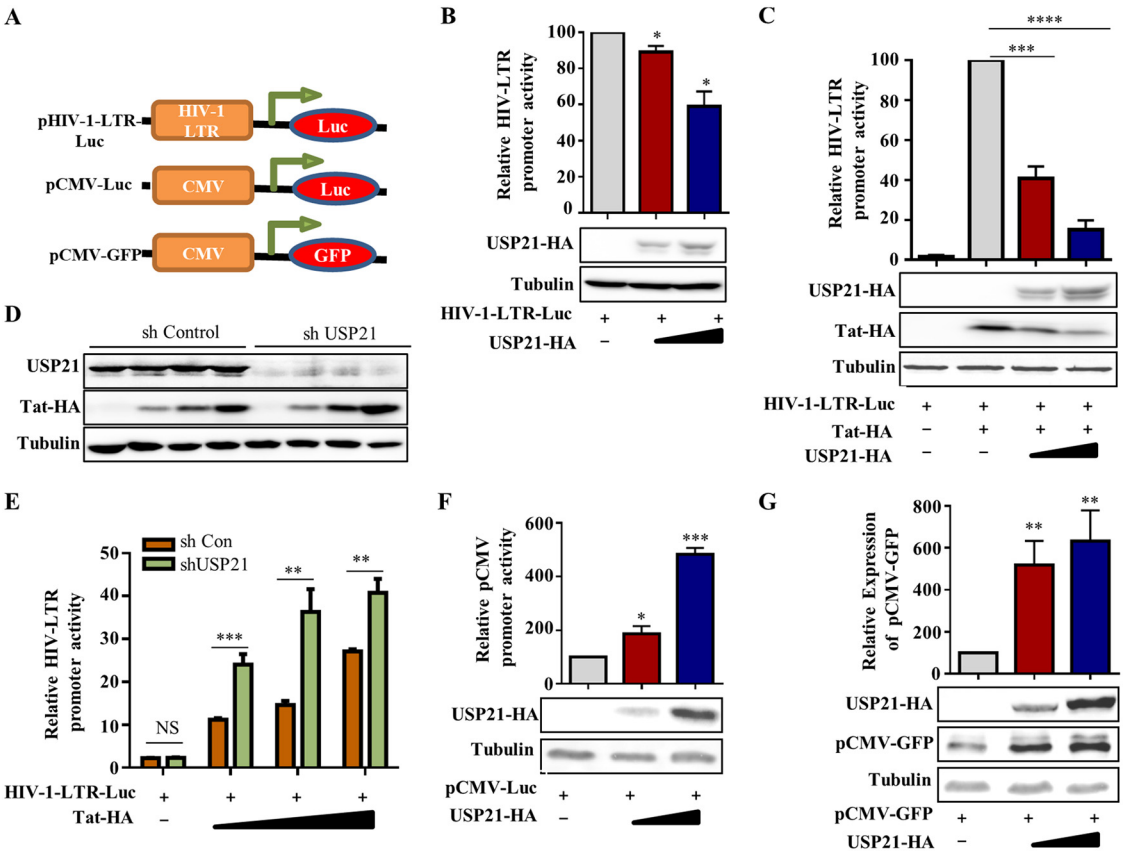

FIG 4 USP21 inhibits Tat-mediated HIV-1 LTR transactivation but not CMV promoter. (A) Schematic representation of the promoter used in the study. (B and C) USP21 affects HIV-1 LTR activity in HEK293T cells. HIV-1 LTR-luciferase, pRenilla, and USP21 plasmids were cotransfected without Tat (B) or with Tat (C) into HEK293T cells. HIV-1 LTR activity was determined using a dual-luciferase reporter assay at 48 h posttransfection, and the cell lysates were immunoblotted with the corresponding antibodies. (D and E) Knockdown of USP21 increased HIV-1 LTR activity in HEK293T cells. HIV-1 LTR-luciferase, Tat, and pRenilla plasmids were cotransfected into negative-control or USP21 knockdown HEK293T cells. HIV-1 LTR activity was determined using a dual-luciferase reporter assay at 48 h posttransfection, and cell lysates were immunoblotted with the corresponding antibodies. (F and G) USP21 increased CMV promoter activity in HEK293T cells. (F) pCMV-luc and USP21 expression vectors were cotransfected into HEK293T cells. pCMV-luc activity was determined using a dual-luciferase reporter assay at 48 h posttransfection, and cell lysates were immunoblotted with the corresponding antibodies. (G) pCMV-GFP and USP21 expression vectors were cotransfected into HEK293T cells. Cell lysates were immunoblotted with the corresponding antibodies. GFP expression was quantified using Image J software to calculate the values relative to that of tubulin. Results are representative of data from three independent experiments. Statistical significance was analyzed using two-sided unpaired *t* tests (NS, not significant; *, $P < 0.05$; **, $P < 0.01$; ***, $P < 0.001$; ****, $P < 0.0001$).

added, including the proteasome inhibitor MG132, NEDD8-activating enzyme (NAE) inhibitor MLN4924, and the autophagolysosomal inhibitor ammonium chloride (NH_4Cl). These inhibitors did not restore the inhibitory effect of USP21 on HIV-1 production (Fig. 3G and H), indicating that USP21 reduced HIV-1 production independent of the proteasome and lysosome pathways.

USP21 specifically suppresses Tat-mediated HIV-1 LTR transactivation by reducing Tat expression. The HIV-1 LTR drives transcriptional initiation and elongation of HIV-1 transcripts. Tat interacts with the TAR element present at the 5′ end of all viral transcripts and stimulates transcriptional elongation. To examine the effect of USP21 on HIV-1 LTR transactivation in the absence or presence of Tat, we used a luciferase reporter system to detect the HIV-1 (HIV-1 LTR) and cytomegalovirus (CMV) promoter activities (Fig. 4A). In the absence of Tat, USP21 had a slight inhibitory effect on HIV-1 LTR activity (Fig. 4B). In the presence of Tat, HIV-1 LTR transactivation was significantly activated (Fig. 4C, lane 2; $P < 0.0001$), whereas USP21 significantly inhibited Tat-driven luciferase activity in a dose-dependent manner (Fig. 4C, lanes 3 and 4; $P < 0.0001$). Interestingly, we observed that the expression of Tat was also

decreased by USP21, which suggests that USP21-mediated inhibition of HIV-1 LTR transactivation is due to reduced Tat expression. Knockdown of USP21 in HEK293T cells increased Tat expression and Tat-mediated HIV-1 LTR activation (Fig. 4D and E). To examine the possible nonspecific effects of USP21 on the promoter, we coexpressed increasing amounts of USP21 with pCMV-luci (Fig. 4F) or pCMV-GFP (Fig. 4G). The results showed that USP21 increased CMV-driven luciferase activity as well as green fluorescent protein (GFP) expression (Fig. 4F and G), indicating that the decreased Tat expression by USP21 was specific.

USP21 downregulates Tat expression by deubiquitinating Tat. We next sought to determine whether USP21 affects mRNA levels of Tat by analyzing the effect of USP21 in cell lines that stably expressed Tat. In HEK293T cells stably expressing Tat, USP21 decreased the protein levels of Tat (Fig. 5A) but did not show a statistically significant reduction in mRNA levels (Fig. 5B), indicating that the downregulation of Tat caused by USP21 occurs at the protein level. It has been reported that Tat ubiquitination is essential for its transcriptional activity (24, 31, 32); therefore, we next examined the effect of deubiquitination on Tat stability. As a DUB, we observed that USP21 clearly reduced the extent of both K48-linked and K63-linked ubiquitination, which is important for Tat transcriptional activity (Fig. 5C), indicating that USP21-induced deubiquitination of Tat causes Tat instability and inhibits Tat-driven LTR activity. We next used a dominant-negative ubiquitin mutant (Ub-KO-Flag), in which all seven lysine residues were mutated to arginine, to detect its effect on Tat stability (33). The results showed that Ub-KO clearly reduced Tat expression, whereas USP21 showed a stronger ability to reduce Tat expression than Ub-KO (Fig. 5D). To confirm that the ubiquitinase activity of USP21 is required for Tat deubiquitination, we examined the effect of a deubiquitinase-deficient mutant (C221A). As expected, the C221A mutant lost the ability to deubiquitinate K48-linked and K63-linked Tat ubiquitination (Fig. 5E). These data support the notion that Tat ubiquitination is important for its stability.

USP21-mediated downregulation of cyclin T1 expression also contributes to reduced Tat expression. Since USP21 had a stronger effect on Tat downregulation than UB-KO (Fig. 5D, lanes 2 and 3), we speculated that USP21 has targets or mechanisms to induce Tat instability other than its effect on Tat ubiquitination. Tat specifically interacts with the positive transcription elongation factor b (P-TEFb) complex, composed of CycT1 and CDK9, that stimulates HIV-1 transcriptional elongation (Fig. 6A). As a previous study reported that CycT1 stabilizes HIV-1 Tat expression (28), we also examined the effect of USP21 on P-TEFb expression as well as Tat-P-TEFb interaction. As reported, CycT1 specifically interacted with Tat in immunoprecipitation (IP) assays using anti-Myc beads and increased Tat expression (data not shown). Interestingly, we observed that USP21 also reduced CycT1 expression in a dose-dependent manner but moderately increased the protein levels of CDK9 upon ectopic expression of CycT1 and CDK9 (Fig. 6B). Accordingly, USP21 silencing increased the protein and mRNA levels of endogenous CycT1 but slightly reduced the protein levels of endogenous CDK9 and had no effect on mRNA levels of endogenous CDK9 (Fig. 6C and D). The efficiency of USP21 knockdown was confirmed by IB and reverse transcription-PCR (RT-PCR) analyses (Fig. 6C and D). Moreover, increasing the amount of CycT1 restored the expression of Tat and promoted LTR-driven luciferase activity, even in the presence of USP21 (Fig. 6E). Accordingly, USP21 knockdown enhanced Tat-mediated LTR activation (Fig. 6F, lane 4), and CycT1 knockdown attenuated Tat-mediated LTR activation (Fig. 6F, lane 6), whereas Tat-mediated LTR activation induced by USP21 knockdown was lost when CycT1 was knocked down (Fig. 6F, lane 8).

Deubiquitinase activity of USP21 is required for HIV-1 inhibition and Tat downregulation. To examine whether USP21-mediated inhibition of HIV infection is related to its deubiquitinase activity, the HIV-1 NL4-3 infectious clone was cotransfected with USP21 WT or a deubiquitinase-deficient mutant (C221A) into HEK293T cells. Overexpression of USP21 WT significantly reduced the expression of intracellular HIV-1 Gagp55 and CAp24 in the supernatant as well as HIV-1 production, measured using TZM-bl indicator cells (Fig. 7A and B, lane 2; $P = 0.0029$), whereas the USP21

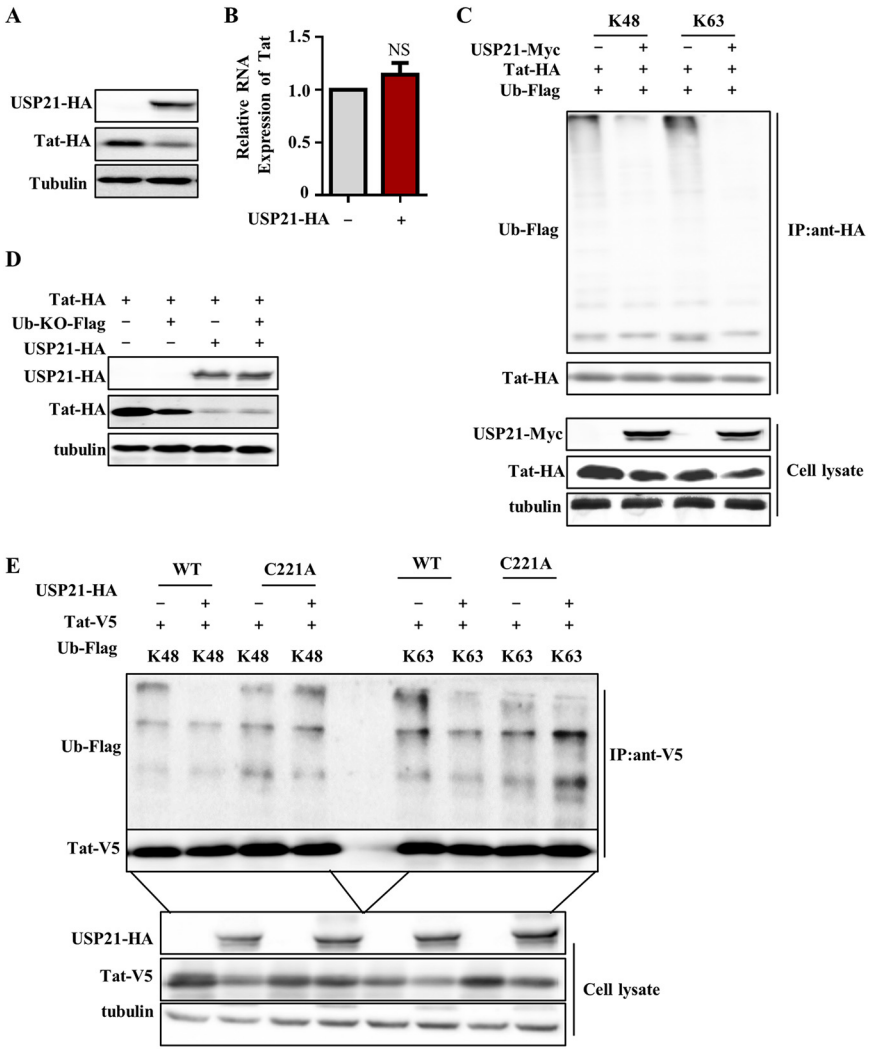

FIG 5 HIV-1 inhibition by USP21 is closely associated with its deubiquitinase activity. (A and B) USP21 reduced Tat expression in cell lines stably expressing Tat. HEK293T cells stably expressing Tat were transfected with USP21 expression vector. After 48 h, cells were harvested for IB (A) and qRT-PCR (B) analyses. mRNA level of Tat in the absence of USP21 was set to 1. qRT-PCR detected Tat mRNA levels. (C) USP21 downregulates Tat ubiquitination. HEK293T cells were transfected with Tat-HA, USP21-Myc, Ub-K48-Flag, or Ub-K63-Flag. Cell lysates were immunoprecipitated with anti-HA antibodies conjugated to agarose beads. Cell lysates and precipitated samples were analyzed by IB with the corresponding antibodies. (D) Ub-KO reduced Tat stability. Tat, Ub-KO, and USP21 expression vectors were transfected into HEK293T cells as described for panels A and B. After 48 h, the cells were harvested and analyzed by IB. (E) USP21 deubiquitinase activity is required for Tat deubiquitination. HEK293T cells were transfected with indicated expression vectors. Cell lysates were immunoprecipitated with anti-V5 antibodies conjugated to agarose beads 48 h later. Cell lysates and precipitated samples were analyzed by IB with the corresponding antibodies.

C221A mutant resulted in a 50% reduction in the expression of HIV-1 viral proteins and HIV-1 yield (Fig. 7A and B, lane 3). To further validate whether the deubiquitinase activity of USP21 is involved in HIV-1 inhibition, we compared the effect of USP21 WT and C221A mutant on Tat expression and HIV-1 LTR transactivation. The USP21 C221A mutant was also defective in Tat downregulation and inhibition of LTR activity compared to USP21 WT (Fig. 7C and D). Neither USP21 WT nor its mutant had any significant cellular toxicity compared to the empty vector (Fig. 7E), indicating that USP21 function was not due to its cytotoxicity. We next examined whether the USP21 C221A mutant affected CycT1 expression. As expected, we found that the USP21 C221A mutant also lacked the ability to reduce the expression of CycT1 (Fig. 7F). Colocalization assays

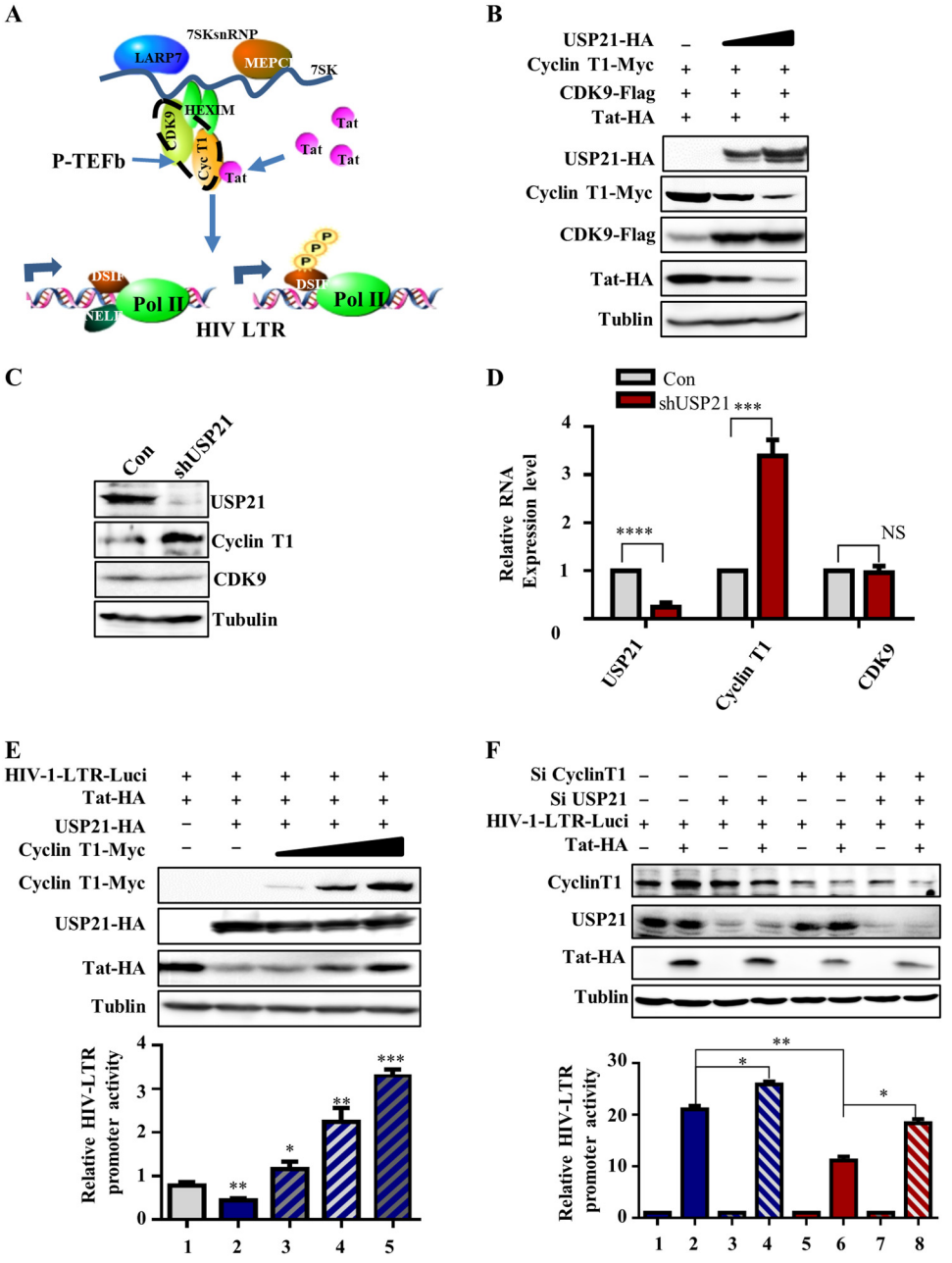

FIG 6 USP21 inhibits Tat expression by reducing cyclin T1 (CycT1) mRNA levels. (A) The model of the P-TEFb complex. (B to D) USP21 inhibited Tat expression by reducing CycT1 mRNA/protein levels. (B) USP21 specifically reduced CycT1 expression. CycT1, CDK9, Tat, and USP21 expression vectors were transfected into HEK293T cells. After 48 h, cells were harvested and analyzed by IB. (C) Knockdown of USP21 increased endogenous CycT1 protein levels in HEK293T cells. (D) USP21, CycT1, and CDK9 mRNA expression in knockdown USP21 cells was detected by qRT-PCR. (E) Increasing CycT1 expression restored Tat expression and counteracted USP21 inhibition on HIV-1 LTR activity. HEK293T cells were transfected with expression vectors as indicated. The cell lysates were immunoblotted with the corresponding antibodies. HIV-1 LTR activity was determined using a dual-luciferase reporter assay. (F) Knockdown of USP21 enhanced Tat-mediated LTR transactivation. HEK293T cells were transfected with USP21- or CycT1 short interfering RNA and expression vectors as indicated. The cell lysates were analyzed by IB, and HIV-1 LTR activity was determined using a dual-luciferase reporter assay. All data are representative of three independent experiments. The data are presented as the means ± SD. (NS, not significant; *, $P < 0.05$; **, $P < 0.01$; ***, $P < 0.001$; ****, $P < 0.0001$).

showed that USP21 WT was distributed both in the cytoplasm and nucleus and colocalized with CycT1 mainly present in the nucleus, whereas the USP21 C221A mutant was mainly localized in the cytoplasm (Fig. 7G); therefore, it could not colocalize with CycT1, resulting in its defective CycT1 downregulation. Taken together, these data

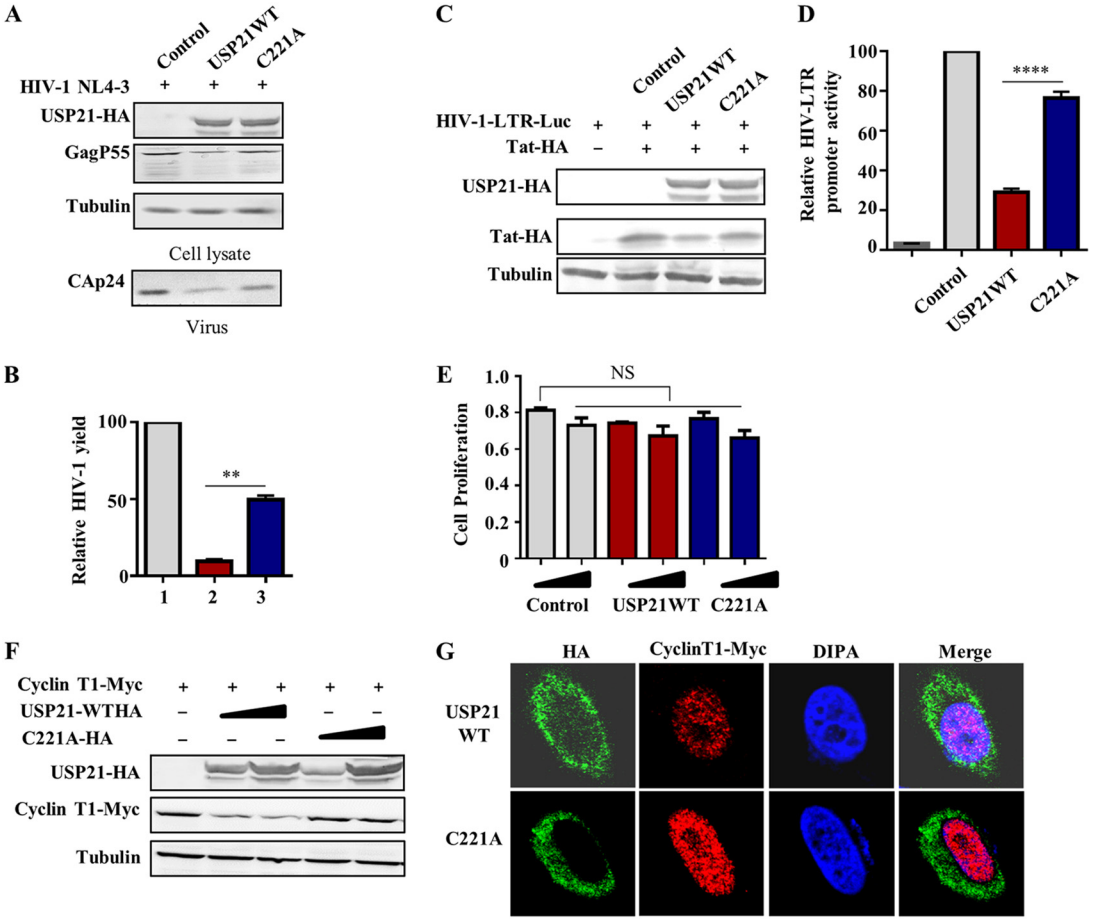

FIG 7 USP21 C221A mutant is defective in HIV-1 inhibition and mainly localizes in the cytoplasm. (A and B) USP21 C221A mutant was defective in HIV-1 inhibition. USP21 WT or USP21 C221A mutant expression vectors were transfected with the HIV-1 expression vector into HEK293T cells. After 48 h, cells and supernatants were harvested and analyzed by IB (A), and HIV-1 viral yield was assessed using TZM-bl indicator cells. (B) The corresponding value of the control was set as 1 or 100% as appropriate. (C) USP21 C221A mutants lost their ability to inhibit HIV-1 LTR activity. HEK293T cells were transfected with expression vectors as indicated. Cell lysates were immunoblotted with the corresponding antibodies. HIV-1 LTR activity was determined using a dual-luciferase reporter assay. (D) Cytotoxicity assays indicated that USP21 and its mutants are not toxic to HEK293T cells. (E) Cytotoxicity assays indicating that USP21 and its mutants are not toxic to HEK293T cells. (F) USP21 C221A mutant was defective in downregulation of CycT1 expression. USP21 WT or USP21 C221A mutant expression vectors were transfected along with the cycT1 into HEK293T cells. After 48 h, the cell lysates were analyzed by IB. (G) USP21 WT but not USP21 C221A mutant colocalized with CycT1. Images were taken with a Zeiss LZM710 confocal microscope. Bars, 10 μm. All data are representative of three independent experiments. The data are presented as means $\pm$ SD. (NS, not significant; ****, $P < 0.0001$).

suggest that USP21 affects Tat expression through deubiquitinating Tat and downregulating CycT1 expression that is necessary for Tat stability.

USP21 reduces CycT1 expression by epigenetically modifying CycT1 promoter. To explore how USP21 reduces CycT1 expression, we first examined whether the UPS is involved in CycT1 downregulation by USP21. We found that the proteasome inhibitor MG132, the NEDD8-activating enzyme (NAE) inhibitor MLN4924, and the autophagolysosomal inhibitor NH_4Cl had no effect on USP21-mediated CycT1 downregulation, indicating that CycT1 downregulation by USP21 does not involve the ubiquitination machinery (Fig. 8A). We next investigated the effect of USP21 on the promoter of CycT1 by constructing a CycT1-Luc expression vector (Fig. 8B). The results showed that USP21 affects the activity of the CycT1 promoter (Fig. 8C). Based on the University of California Santa Cruz (UCSC) Genome Browser analysis, we found that the CycT1 promoter has epigenetic modifications, including histone 3 K4 and K9 methylation (H3K4me3, H3K9me3) and histone 3 K27 acetylation (H3K27ac). Chromatin

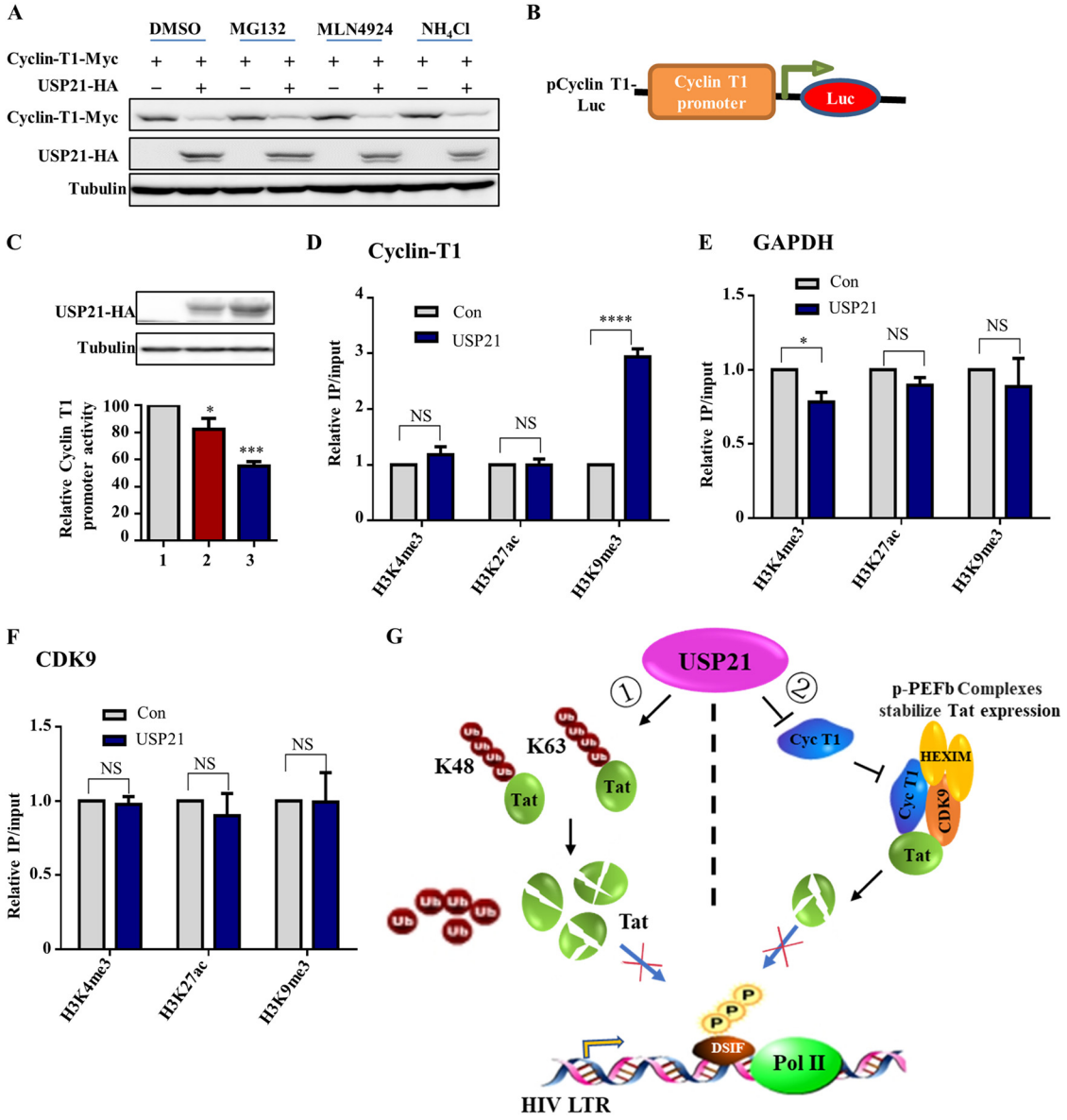

FIG 8 Proposed model of USP21-mediated inhibition of HIV-1. (A) USP21 reduced CycT1 expression independent of proteasome degradation. CycT1 was cotransfected along with VR1012 or USP21 into cells for 24 h, and the cells were then treated with 10 μM MG132, 1 μM MLN4924, and 20 μM NH_4Cl for 12 h before harvest. The cell lysates were immunoblotted with the corresponding antibodies. (B) Construction of CycT1 promoter with the luciferase reporter construct. (C) USP21 reduced CycT1 promoter activity. CycT1 promoter was cotransfected along with VR1012 or USP21 for 48 h, and the cell lysates were analyzed by IB. Cyclin T1 promoter activity was determined by using a dual-luciferase reporter assay. (D) USP21 expression increased the histone H3 (trimethyl K9) mark on the CycT1 promoter, as revealed by anti-H3K9Me3, anti-H3K4me3, and anti-H3K27ac ChIP assays in HEK293T cells showing the level of H3K9Me3 in the CycT1 promoter following transfection with USP21 expression vector or empty vector. (E and F) USP21 expression did not affect the H3K9 methylation mark on the GAPDH and CDK9 promoters. (G) Proposed inhibitory mechanism of USP21 on HIV-1 production occurs through downregulation of Tat expression via two mechanisms. First, USP21 deubiquitinates polyubiquitinated Tat, resulting in Tat instability, and second, USP21 reduces mRNA levels of CycT1, an important component of P-TEFb that results in downregulation of Tat.

immunoprecipitation (ChIP) assay showed that USP21 expression clearly increased H3K9 methylation but had no effect on H3K4 methylation or H3K27 acetylation (Fig. 8D), which led to decreased CycT1 expression. Moreover, we found that USP21 did not affect the H3K9 methylation mark on the glyceraldehyde-3-phosphate dehydrogenase (GAPDH) and CDK9 promoters (Fig. 8E and F), indicating that the effect on the promoter of CycT1 is specific. Collectively, these results suggest that USP21 is a novel regulator of HIV-1 production, and the regulation is associated with USP21 deubiquitinase activity.

DISCUSSION

Numerous studies have demonstrated that the UPS is an important regulatory mechanism in viral infection. The UPS is composed of three main components, including the proteasome holoenzymes, various ubiquitin ligases, and deubiquitinating enzymes (34). It is well known that viruses, especially HIV-1, manipulate the host proteasomal machinery for its propagation and pathogenesis. HIV-1-encoded Vif, Vpr, Vpu, and Nef proteins recruit different host factors, such as Cullin5-ElonginB/C-CBF-β-Rbx or VprBP-Cullin4A-DCAF-1-DDB-1-Rbx1, to form E3 ligase and to counteract the host restriction factors APOBEC3, CTIP2, UNG2, HLTF, Dicer, BST-2, SERINC3, and SERINC5 and even regulate viral protein Tat expression through the proteasomal pathway (8). Ubiquitination is a dynamic and reversible process in eukaryotic cells; therefore, the role of deubiquitination, mediated by DUBs, has attracted intense scrutiny and has recently been demonstrated.

In the present study, we demonstrated that the DUB USP21 inhibits HIV production by specifically targeting Tat protein (Fig. 2 and 4) without affecting Vif, Vpr, Vpx, and Vpu functions (Fig. 3). USP21 specifically reduced Tat expression, resulting in a defect in HIV-1 LTR transactivation (Fig. 4), eventually inhibiting HIV-1 production (Fig. 2). USP21 not only caused Tat deubiquitination via its deubiquitinase activity (Fig. 5) but also downregulated CycT1 mRNA levels through epigenetic modification of the CycT1 promoter (Fig. 6 and 8). Decreased CycT1 affects the stability of HIV-1 Tat protein (28). Although the deubiquitinase activity of USP21 is closely associated with its inhibition of HIV-1 infection (Fig. 7), two different mechanisms may be involved (Fig. 8G). The deubiquitinase activity of USP21 plays a major role in deubiquitinating Tat, whereas localization is involved in downregulating CycT1 mRNA levels; the localization of USP21 deubiquitinase-deficient mutant C221A, mainly in the cytoplasm, reduces its capacity to downregulate CycT1, which further supports our conclusion that nuclear localization of USP21 specifically leads to increased H3K9 methylation of the CycT1 promoter, thereby downregulating CycT1 (Fig. 7 and 8). However, there is an interesting phenomenon that USP21 also reduces the expression of exogenous CycT1 (Fig. 6 and 7), which is not due to the effect on the promoter of the exogenous plasmid (data not shown). Because the *Cyclin-T1* gene contains a complex promoter that exhibits an extreme degree of functional redundancy (35), whereas USP21 has a powerful function that regulates gene expression or transcription through phosphorylation, acetylation, deubiquitination, or sumoylation (36), our finding that USP21 reduced cyclin T1 expression through affecting the H3K9 methylation mark on the cyclin T1 promoters might only be one aspect. Other mechanisms exist that we have not found, which might be worth investigating in the future. Our findings revealed a novel function of USP21 in the nucleus. USP21 has been reported to be involved in multiple cellular functions, such as the regulation of cell cycle progression, cell proliferation and metastasis, tumor occurrence, and virus infection (17, 37–39). USP21 also regulates transcription; for example, USP21 is a positive regulator of the transcription factor GATA3 via its deubiquitination (40). BEND3 represses rRNA gene transcription by stabilizing an NoRC component via association with USP21 (41). USP21 recruits and stabilizes Gli1, the key transcription factor required for Hh signal amplification at the centrosome, by promoting PKA-dependent phosphorylation of Gli1 (36). The molecular mechanisms by which USP21 regulates CycT1 are interesting and need to be further investigated in the future.

From the experimental evidence that USP21-mediated deubiquitination of Tat caused Tat instability, we unexpectedly found that Tat polyubiquitination is required for Tat stability and transcriptional activity, which was further confirmed by a Ub-KO-induced decrease in Tat expression (Fig. 5D). This phenomenon is consistent with a previous report that nonproteolytic ubiquitination of Tat is important for Tat-mediated transactivation (24). Tat is not only required for HIV-1 transcription and viral gene expression but also contributes to HIV-1 latency. Insufficient Tat or Tat overexpression

causes HIV-1 latency or stimulates latent HIV-1 reactivation, respectively. Therefore, whether USP21 regulates HIV-1 latency is worth further investigation.

To summarize, we found that USP21 restricts HIV-1 production by reducing HIV-1 Tat. Recent evidence indicates that targeting the UPS is effective for the treatment for certain cancers (42, 43). Therefore, USP21 may be an important target for drug development or novel therapeutic strategies against HIV-1.

MATERIALS AND METHODS

Plasmid construction. All USPs with the hemagglutinin (HA)-Flag tag were purchased from Addgene (Watertown, MA, USA). USP21-HA was constructed with a C-terminal HA tag and inserted between the SalI and BamHI sites of VR1012. USP21-HA C221A was made from USP21-HA by site-directed mutagenesis. HLTF-HA was constructed with seamless assembly cloning kit and inserted into VR1012. pHIV-1 LTR-luci, pCMV-GFP, Renilla, and pCMV-luci were as described previously (44). The cyclin T1 promoter, between −1027 and +1 bp upstream of the cyclin T1 transcription start site, was constructed. cyclin T1 promoter −1027/+1 luciferase (pCyclin-T1-luc) plasmid was amplified with the corresponding fragment from human genomic DNA, and then the fragments were ligated and cloned into the pGL3 basic vector. pEF-Cyclin-T1-Myc was purchased from Addgene (number 14626). Tat-HA was subjected to gene synthesis by Shanghai Generay Biotech Co., Ltd. (Shanghai, China). The infectious molecular clone pNL4-3 (HIV-1 WT) was obtained from the AIDS Research and Reference Reagents Program, Division of AIDS, National Institute of Allergy and Infectious Diseases (NIAID), National Institutes of Health (NIH). The expression vectors A3G-HA and HIV-1 NL4-3-Vif-HA (Vif-HA) (4), HIV-2_{Rod}Vpx and SAMHD1-HA (45), and Vpu-HA and BST-2-HA (46) were described previously, and Vpr-HA and HLTF-Flag were constructed by our laboratory as described previously (47). The *SAMHD1* gene with a C-terminal Myc tag was amplified using SAMHD1-HA as the template and was cloned into the VR1012-Entry vector via the SgII and BamHI sites.

RNA extraction and quantitative real-time qRT-PCR. RNA was isolated with TRIzol reagent by following the manufacturer's instructions (15596-026; Invitrogen, Carlsbad, CA, USA). Before reverse transcription, RQ-1 DNase (Promega, Madison, WI, USA) was used to treat RNA samples. cDNA synthesis was performed using EasyScript first-strand cDNA synthesis supermix (AE301; TransGen Biotech, Beijing, China) according to the manufacturer's instructions. A total of 250 to 1,000 ng of total RNA was used as a template for each cDNA synthesis reaction, and samples containing only H_2O or no reverse transcriptase were included as blank samples. cDNA was stored at −80°C until use. The quantitative real-time PCR (qPCR) was carried out on an Mx3005P instrument (Agilent Technologies, Stratagene, USA) using the Power SYBR green PCR master mix (2×) (4367659; ABI). Quantitative RT-PCR (qRT-PCR) amplification of the target fragment was carried out with initial activation at 95°C for 2 min, followed by 45 cycles at 95°C for 15 s, 57°C for 15 s, and 68°C for 20 s. The primers used in this study are listed below: GAPDH-F, GCAAATTCCATGGCACCGT; GAPDH-R, TCGCCCCACTTGATTTTGG; USP21-F, ATTCCGAGCTGTCTTCCAGA; USP21-R, CATTAGGTTGGCTCGGTCAT; CycT1-F, GTCCCTCATTCGAAACTGGA; CycT1-R, GTTCTGATGGCAGAGGTGGT. Data were normalized to the housekeeping GAPDH gene, and the relative abundance of the transcripts was calculated by the threshold cycle (C_T) models.

Cell culture, transfection, and antibodies. HEK293T (CRL-11268; ATCC), HeLa (CRM-CCL-2; ATCC), and TZM-bl (PTA-5659; ATCC) cells were obtained from the American Type Culture Collection (ATCC; Manassas, VA, USA) and maintained in Dulbecco's modified Eagle's medium (DMEM; HyClone, Logan, UT, USA) containing 10% heat-inactivated fetal bovine serum (FBS; 04-001-1; Biological Industries) and 100 μg/ml penicillin-streptomycin, and Jurkat (TIB-152; ATCC) cells were maintained in RPMI 1640 medium with 10% fetal calf serum and 100 μg/ml penicillin-streptomycin. DNA transfections were carried out by Lipofectamine 2000 (Invitrogen) according to the manufacturer's instruction. The antibodies used in this study are listed below. Anti-HA (901513) monoclonal antibody (MAb) and anti-Tat (MMS-116P) MAb were purchased from BioLegend (San Diego, CA, USA). Anti-Myc (AHO0052) MAb and anti-GFP polyclonal antibody (A-21311) were purchased from Invitrogen. Anti-USP21 (17856-1-AP) rabbit polyclonal antibody and anti-CycT1 (20991-1-AP) rabbit polyclonal antibody were purchased from Proteintech (Rosemont, IL, USA). Rabbit polyclonal antibody to histone H3 (trimethyl K4) (ab8580), rabbit polyclonal antibody to histone H3 (acetyl K27) (ab4729), rabbit polyclonal antibody to histone H3 (tri-methyl K9) (ab8898), and anti-CDK9 (ab76320) were purchased from Abcam (Cambridge, MA, USA). Anti-CAp24 MAb (1513) was purchased from the NIH AIDS Reagents Program. Anti-tubulin mouse monoclonal antibody was obtained from Beijing Ray Antibody Biotech (number RM2002; Beijing, China). Secondary antibodies were alkaline phosphatase-conjugated anti-rabbit (115–055–045) and anti-mouse (115–055–062) and were purchased from Jackson (West Grove, PA, USA). Alexa Fluor 488 goat anti-rabbit IgG (A-11034) and Alexa Fluor 555 goat anti-mouse IgG2a (A-21137) were purchased from Thermo Fisher (Waltham, MA USA). All antibodies were used by following the manufacturer's protocols.

Immunoblot analysis. For immunoblot analysis of cell-associated proteins, whole-cell lysates were prepared as follows. Cells were lysed by buffer (50 mM Tris-HCl, pH 7.8, 150 mM NaCl, 1% NP-40, 1% sodium deoxycholate, 4 mM EDTA) and boiled in 1× loading buffer (0.08 M Tris [pH 6.8], 2.0% SDS, 10% glycerol, 0.1 M dithiothreitol, and 0.2% bromophenol blue) at 100°C with occasional vortexing to shear cellular DNA. Cell lysates were subjected to SDS-PAGE. Proteins were transferred to nitrocellulose (NC) membranes (10401396; GE Whatman, USA) and reacted with appropriate antibodies as described in the text. The membranes incubated with HRP-conjugated secondary antibody (Jackson) then were visualized using the ultrasensitive ECL chemiluminescence detection kit (B500024; Proteintech).

Cell proliferation assay. HEK293T cells seeded onto 24-well plates were transfected with empty vector or USP21 (300 or 600 ng). After 48 h posttransfection, the cells were reseeded onto a 96-well plate, and 10 ml of cell counting kit-8 (CCK; Transgen Biotech, Beijing, China) reagent was added to each well. After a further 1 h, the absorption of the samples was examined at 450 nm with an iMark Macroplate (Bio-Rad, Hercules, CA, USA). DMEM (containing 10% FBS) was used as a negative control to control for background noise.

HIV-1 production and infection. HIV-1 was produced by transfecting pNL4-3 plasmids into HEK293T cells with Lipofectamine 2000 (Invitrogen) according to the manufacturer's instructions. Forty-eight hours later, supernatants were collected, and HIV-1 was quantified using an HIV-1 p24 enzyme-linked immunosorbent assay kit (Hebei Medical University, China).

TZM-bl cells containing an integrated HIV-1 LTR promoter, which were derived from HeLa cells, were used to assess infectious HIV-1 production. TZM-bl cells were seeded in a 24-well plate overnight and then were infected with supernatant containing HIV-1 particles in a total volume of 20 μl in the presence of 20 μg/ml DEAE. Forty-eight hours postinfection, the infected cells were harvested, and luciferase activity was measured with a GloMax 20/20 luminometer (Promega).

Lentiviral production, transduction, and infection. Lentiviruses were produced by transfection of HEK293T cells with pLKO.1-sh control or pLKO.1-shUSP21 (sh control, 5′-CAACAAGATGAAGAGCACCAA-3′; sh human USP21, 5′-CCACTTTGAGACGTAGCACTT-3′) together with pRSV-Rev, pMDLg/pRRE, and pCMV-VSVG. The assembled virus-like particles (VLPs) in the culture supernatants were used to infect fresh HEK293T cells. Forty-eight hours postinfection, HEK293T cells were selected with 5 μg/ml puromycin (P8833; Sigma, St. Louis, MO, USA), USP21 expression of mRNA level was monitored by RT-PCR, and protein level was assessed by immunoblotting. For stable overexpressed Tat-HA HEK293T cell lines, pLVX-Tat-HA vector was used in the same way.

Luciferase assay. For promoter activity, HEK293T cells were precultured in a 12-well cell culture plate and transfected using Lipofectamine 2000 according to the manufacturer's instructions. The cells were collected and lysed after 48 h. Luciferase activity was measured with the Dual-Luciferase reporter assay system (E1910; Promega) according to the manufacturer's protocol with the GloMax 20/20 luminometer.

ChIP. Chromatin immunoprecipitation (ChIP) was performed using a ChIP kit (26157; Thermo), and a total of 4×10^6 cells were used for each ChIP assay. Briefly, 293T cells were transfected with USP21 expression or negative-control vector for 48 h. For cross-linking the proteins to DNA, the transfected cells were treated with 1% formaldehyde (Sigma) for 10 min at room temperature (23 to 27°C). Unreacted formaldehyde was quenched with 125 mM glycine for 5 min at room temperature (23 to 27°C). Cells were washed twice with one medium volume of ice-cold phosphate-buffered saline (PBS), and the supernatant was removed by aspiration. Next, 1 ml ice-cold PBS containing 1× protease inhibitor cocktail II was added to the cells, and the cells were detached by scraping. The cell suspension was transferred to a 1.5-ml microcentrifuge tube using a pipette and centrifuged at 3,000 × *g* for 5 min. The cells were resuspended in 200 μl of MNase digestion buffer working solution containing 2 μl MNase, and the tubes were vortexed and incubated in a 37°C water bath for 15 min with intermittent mixing by inverting the tubes every 5 min. The cell lysates then were sonicated on ice with three sets of 6-s pulses using a Cole-Parmer instrument to obtain DNA fragments of appropriate sizes between 150 and 900 bp and centrifuged at 9,000 × *g* for 10 min at 4°C. The supernatants were collected and precleared by incubation with normal rabbit IgG, followed by incubation with anti-H3K4me3 antibody, anti-H3K27ac antibody, or anti-H3K9me3 antibody overnight at 4°C with mixing. ChIP-grade protein G magnetic beads were mixed to obtain a uniform suspension, and 20 μl of beads was added to each IP and incubated for 2 h at 4°C with mixing. The beads were collected using a magnetic stand, and the supernatant was carefully removed and discarded. The beads were then washed twice with IP wash buffer 1 and once with IP wash buffer 2. For elution, the beads were suspended in 150 μl of 1× IP elution buffer containing NaCl and proteinase K, followed by incubation at 65°C for 1.5 h to reverse the DNA-protein cross-links. The DNA was recovered by adding 750 μl of DNA binding buffer to each eluted IP and total input sample. Each sample (500 μl) was then pipetted into DNA cleanup columns inserted into 2-ml collection tubes. The columns were centrifuged at 10,000 × *g* for 1 min, and the flowthrough was discarded. The remaining sample was pipetted into the same DNA cleanup column, the columns were centrifuged at 10,000 × *g* for 1 min, and the flowthrough was discarded. The column was placed back into the collection tube, and 750 μl of DNA column wash buffer was added. The columns were then centrifuged at 10,000 × *g* for 1 min and the flowthrough was discarded. The column was placed in a new 1.5-ml centrifuge tube, and 50 μl of DNA column elution solution was pipetted directly into the center of each column. The column was centrifuged at 10,000 × *g* for 1 min. The eluted solution contained the purified DNA that was detected using qPCR. The specific procedure was carried out according to the product manual. The primers used in the ChIP assay are the following: Cyc-T1 F2-RT, 5′-CAAAACGACGGGATGGGCTA-3′; Cyc-T1 R2-RT, 5′-TTAGGTGACGCTGGGAAGTG-3′; CDK9 promoter-RT-F, 5′-TCCCAGGGCCGGAGG-3′; CDK9 promoter-RT-R: 5′-TGCAGCGGAAAGCCCC-3′; GAPDH promoter RT-F, 5′-CCAATTCCCCATCTCAGTCGT-3′; GAPDH promoter RT-R, 5′-GTCAAGGACGGGGACCCTTA-3′.

Immunofluorescence. USP21 WT or its mutant plus with CycTI-Myc were transfected into HeLa cells grown on glass coverslips. At 24 h after transfection, the cells were fixed with 4% paraformaldehyde for 20 min at ambient temperature and then washed three times with PBS, followed by a 10-min permeabilization with 0.25% Triton X-100, also at ambient temperature. Cells were then incubated for 2 h at ambient temperature with HA antibody, followed by fluorescent Alexa Fluor 488 goat anti-rabbit IgG and Alexa Fluor 555 goat anti-mouse IgG2a for 2 h at ambient temperature. Fluorescence was then tested,

all images were taken with a 63× objective, and image analysis and manipulation were conducted using Zen 2009 software.

Co-IP. Transfected 293T cells were harvested, lysed in lysis buffer (50 mM Tris at pH 7.5, 150 mM NaCl, 1% NP-40, and complete protease inhibitor cocktail tablets) at 4°C for 1 h and then centrifuged at 10,000 × *g* for 30 min. For HA tag immunoprecipitation, precleared cell lysates were mixed with anti-HA antibody-conjugated agarose beads and incubated at 4°C overnight. The second day, samples were washed six times with washing buffer (20 mM Tris at pH 7.5, 100 mM NaCl, 0.1 mM EDTA, 0.05% Tween 20) and subsequently analyzed by Western blotting or extracted RNA for qRT-PCR analysis.

Statistical analysis. All data represent the results from three independent experiments and are presented as the means ± standard deviations (SD). Statistical significance was calculated using Student's *t* test. Asterisks indicate significant differences: *, $P < 0.05$; **, $P < 0.01$; ***, $P < 0.001$.

ACKNOWLEDGMENTS

We thank C. Y. Dai for critical reagents. We thank the AIDS Research and Reference Reagent Program, Division of AIDS, National Institute of Allergy and Infectious Diseases (NIAID), National Institutes of Health (NIH), for critical reagents.

This work was supported in part by funding from the National Natural Science Foundation of China (81930062 and 81672004 to W.Y.Z. and 31900457 to W.Y.G.), the Science and Technology Department of Jilin Province (20190101003JH, 20200201422JC, and 20190201272JC), the Key Laboratory of Molecular Virology, Jilin Province (20102209), and the Chinese Ministry of Science and Technology (2018ZX10302104-001-010). This work was supported by the Fundamental Research Funds for the Central Universities.

W.Y.Z. and W.Y.G. conceived and designed the experiments, analyzed data, and wrote the manuscript. B.S.Z. and C.L.J. analyzed data. W.Y.G., G.Q.L., S.M.Z., and H.W. performed the experiments. H.C. contributed reagents, materials, and analysis tools.

We have no conflicts of interest to declare.

REFERENCES

1. Goldstone DC, Ennis-Adeniran V, Hedden JJ, Groom HC, Rice GI, Christodoulou E, Walker PA, Kelly G, Haire LF, Yap MW, de Carvalho LP, Stoye JP, Crow YJ, Taylor IA, Webb M. 2011. HIV-1 restriction factor SAMHD1 is a deoxynucleoside triphosphate triphosphohydrolase. Nature 480:379–382. https://doi.org/10.1038/nature10623.
2. Hrecka K, Hao C, Gierszewska M, Swanson SK, Kesik-Brodacka M, Srivastava S, Florens L, Washburn MP, Skowronski J. 2011. Vpx relieves inhibition of HIV-1 infection of macrophages mediated by the SAMHD1 protein. Nature 474:658–661. https://doi.org/10.1038/nature10195.
3. Simon V, Bloch N, Landau NR. 2015. Intrinsic host restrictions to HIV-1 and mechanisms of viral escape. Nat Immunol 16:546–553. https://doi.org/10.1038/ni.3156.
4. Yu X, Yu Y, Liu B, Luo K, Kong W, Mao P, Yu XF. 2003. Induction of APOBEC3G ubiquitination and degradation by an HIV-1 Vif-Cul5-SCF complex. Science 302:1056–1060. https://doi.org/10.1126/science.1089591.
5. Zhang W, Du J, Evans SL, Yu Y, Yu XF. 2011. T-cell differentiation factor CBF-beta regulates HIV-1 Vif-mediated evasion of host restriction. Nature 481:376–379. https://doi.org/10.1038/nature10718.
6. Augustine T, Chaudhary P, Gupta K, Islam S, Ghosh P, Santra MK, Mitra D. 2017. Cyclin F/FBXO1 interacts with HIV-1 viral infectivity factor (Vif) and restricts progeny virion infectivity by ubiquitination and proteasomal degradation of Vif protein through SCF(cyclin F) E3 ligase machinery. J Biol Chem 292:5349–5363. https://doi.org/10.1074/jbc.M116.765842.
7. Izumi T, Takaori-Kondo A, Shirakawa K, Higashitsuji H, Itoh K, Io K, Matsui M, Iwai K, Kondoh H, Sato T, Tomonaga M, Ikeda S, Akari H, Koyanagi Y, Fujita J, Uchiyama T. 2009. MDM2 is a novel E3 ligase for HIV-1 Vif. Retrovirology 6:1. https://doi.org/10.1186/1742-4690-6-1.
8. Lata S, Mishra R, Banerjea AC. 2018. Proteasomal degradation machinery: favorite target of HIV-1 proteins. Front Microbiol 9:2738. https://doi.org/10.3389/fmicb.2018.02738.
9. Li J, Chen C, Ma X, Geng G, Liu B, Zhang Y, Zhang S, Zhong F, Liu C, Yin Y, Cai W, Zhang H. 2016. Long noncoding RNA NRON contributes to HIV-1 latency by specifically inducing tat protein degradation. Nat Commun 7:11730. https://doi.org/10.1038/ncomms11730.
10. Weiss ER, Popova E, Yamanaka H, Kim HC, Huibregtse JM, Gottlinger H. 2010. Rescue of HIV-1 release by targeting widely divergent NEDD4-type ubiquitin ligases and isolated catalytic HECT domains to Gag. PLoS Pathog 6:e1001107. https://doi.org/10.1371/journal.ppat.1001107.
11. Clague MJ, Urbe S, Komander D. 2019. Breaking the chains: deubiquitylating enzyme specificity begets function. Nat Rev Mol Cell Biol 20:338–352. https://doi.org/10.1038/s41580-019-0099-1.
12. Gu Z, Shi W. 2016. Manipulation of viral infection by deubiquitinating enzymes: new players in host-virus interactions. Future Microbiol 11:1435–1446. https://doi.org/10.2217/fmb-2016-0091.
13. Wang S, Wang K, Li J, Zheng C. 2013. Herpes simplex virus 1 ubiquitin-specific protease UL36 inhibits beta interferon production by deubiquitinating TRAF3. J Virol 87:11851–11860. https://doi.org/10.1128/JVI.01211-13.
14. Whitehurst CB, Vaziri C, Shackelford J, Pagano JS. 2012. Epstein-Barr virus BPLF1 deubiquitinates PCNA and attenuates polymerase eta recruitment to DNA damage sites. J Virol 86:8097–8106. https://doi.org/10.1128/JVI.00588-12.
15. Yang X, Chen X, Bian G, Tu J, Xing Y, Wang Y, Chen Z. 2014. Proteolytic processing, deubiquitinase and interferon antagonist activities of Middle East respiratory syndrome coronavirus papain-like protease. J Gen Virol 95:614–626. https://doi.org/10.1099/vir.0.059014-0.
16. Cui J, Song Y, Li Y, Zhu Q, Tan P, Qin Y, Wang HY, Wang RF. 2014. USP3 inhibits type I interferon signaling by deubiquitinating RIG-I-like receptors. Cell Res 24:400–416. https://doi.org/10.1038/cr.2013.170.
17. Fan Y, Mao R, Yu Y, Liu S, Shi Z, Cheng J, Zhang H, An L, Zhao Y, Xu X, Chen Z, Kogiso M, Zhang D, Zhang H, Zhang P, Jung JU, Li X, Xu G, Yang J. 2014. USP21 negatively regulates antiviral response by acting as a RIG-I deubiquitinase. J Exp Med 211:313–328. https://doi.org/10.1084/jem.20122844.
18. Wang L, Zhao W, Zhang M, Wang P, Zhao K, Zhao X, Yang S, Gao C. 2013. USP4 positively regulates RIG-I-mediated antiviral response through deubiquitination and stabilization of RIG-I. J Virol 87:4507–4515. https://doi.org/10.1128/JVI.00031-13.
19. Ali A, Raja R, Farooqui SR, Ahmad S, Banerjea AC. 2017. USP7 deubiquitinase controls HIV-1 production by stabilizing Tat protein. Biochem J 474:1653–1668. https://doi.org/10.1042/BCJ20160304.
20. Xu M, Moresco JJ, Chang M, Mukim A, Smith D, Diedrich JK, Yates JR, III, Jones KA. 2018. SHMT2 and the BRCC36/BRISC deubiquitinase regulate HIV-1 Tat K63-ubiquitylation and destruction by autophagy. PLoS Pathog 14:e1007071. https://doi.org/10.1371/journal.ppat.1007071.
21. Pyeon D, Timani KA, Gulraiz F, He JJ, Park IW. 2016. Function of ubiquitin (Ub) specific protease 15 (USP15) in HIV-1 replication and viral protein

degradation. Virus Res 223:161–169. https://doi.org/10.1016/j.virusres.2016.07.009.
22. Pan T, Song Z, Wu L, Liu G, Ma X, Peng Z, Zhou M, Liang L, Liu B, Liu J, Zhang J, Zhang X, Huang R, Zhao J, Li Y, Ling X, Luo Y, Tang X, Cai W, Deng K, Li L, Zhang H. 2019. USP49 potently stabilizes APOBEC3G protein by removing ubiquitin and inhibits HIV-1 replication. Elife 8:e48318. https://doi.org/10.7554/eLife.48318.
23. Faust TB, Binning JM, Gross JD, Frankel AD. 2017. Making sense of multifunctional proteins: human immunodeficiency virus type 1 accessory and regulatory proteins and connections to transcription. Annu Rev Virol 4:241–260. https://doi.org/10.1146/annurev-virology-101416-041654.
24. Bres V, Kiernan RE, Linares LK, Chable-Bessia C, Plechakova O, Treand C, Emiliani S, Peloponese JM, Jeang KT, Coux O, Scheffner M, Benkirane M. 2003. A non-proteolytic role for ubiquitin in Tat-mediated transactivation of the HIV-1 promoter. Nat Cell Biol 5:754–761. https://doi.org/10.1038/ncb1023.
25. Chen S, Yang X, Cheng W, Ma Y, Shang Y, Cao L, Chen S, Chen Y, Wang M, Guo D. 2017. Immune regulator ABIN1 suppresses HIV-1 transcription by negatively regulating the ubiquitination of Tat. Retrovirology 14:12. https://doi.org/10.1186/s12977-017-0338-5.
26. Ali A, Banerjea AC. 2016. Curcumin inhibits HIV-1 by promoting Tat protein degradation. Sci Rep 6:27539. https://doi.org/10.1038/srep27539.
27. Lata S, Ali A, Sood V, Raja R, Banerjea AC. 2015. HIV-1 Rev downregulates Tat expression and viral replication via modulation of NAD(P)H:quinine oxidoreductase 1 (NQO1). Nat Commun 6:7244. https://doi.org/10.1038/ncomms8244.
28. Imai K, Asamitsu K, Victoriano AF, Cueno ME, Fujinaga K, Okamoto T. 2009. Cyclin T1 stabilizes expression levels of HIV-1 Tat in cells. FEBS J 276:7124–7133. https://doi.org/10.1111/j.1742-4658.2009.07424.x.
29. Lahouassa H, Blondot ML, Chauveau L, Chougui G, Morel M, Leduc M, Guillonneau F, Ramirez BC, Schwartz O, Margottin-Goguet F. 2016. HIV-1 Vpr degrades the HLTF DNA translocase in T cells and macrophages. Proc Natl Acad Sci U S A 113:5311–5316. https://doi.org/10.1073/pnas.1600485113.
30. Neil SJ, Zang T, Bieniasz PD. 2008. Tetherin inhibits retrovirus release and is antagonized by HIV-1 Vpu. Nature 451:425–430. https://doi.org/10.1038/nature06553.
31. Zhang L, Qin J, Li Y, Wang J, He Q, Zhou J, Liu M, Li D. 2014. Modulation of the stability and activities of HIV-1 Tat by its ubiquitination and carboxyl-terminal region. Cell Biosci 4:61. https://doi.org/10.1186/2045-3701-4-61.
32. Faust TB, Li Y, Jang GM, Johnson JR, Yang S, Weiss A, Krogan NJ, Frankel AD. 2017. PJA2 ubiquitinates the HIV-1 Tat protein with atypical chain linkages to activate viral transcription. Sci Rep 7:45394. https://doi.org/10.1038/srep45394.
33. Bartkova J, Horejsi Z, Koed K, Kramer A, Tort F, Zieger K, Guldberg P, Sehested M, Nesland JM, Lukas C, Orntoft T, Lukas J, Bartek J. 2005. DNA damage response as a candidate anti-cancer barrier in early human tumorigenesis. Nature 434:864–870. https://doi.org/10.1038/nature03482.
34. Bailey-Elkin BA, Knaap RCM, Kikkert M, Mark BL. 2017. Structure and function of viral deubiquitinating enzymes. J Mol Biol 429:3441–3470. https://doi.org/10.1016/j.jmb.2017.06.010.
35. Martin-Serrano J, Li K, Bieniasz PD. 2002. Cyclin T1 expression is mediated by a complex and constitutively active promoter and does not limit human immunodeficiency virus type 1 Tat function in unstimulated primary lymphocytes. J Virol 76:208–219. https://doi.org/10.1128/jvi.76.1.208-219.2002.
36. Heride C, Rigden DJ, Bertsoulaki E, Cucchi D, De Smaele E, Clague MJ, Urbe S. 2016. The centrosomal deubiquitylase USP21 regulates Gli1 transcriptional activity and stability. J Cell Sci 129:4001–4013. https://doi.org/10.1242/jcs.188516.
37. Arceci A, Bonacci T, Wang X, Stewart K, Damrauer JS, Hoadley KA, Emanuele MJ. 2019. FOXM1 deubiquitination by USP21 regulates cell cycle progression and paclitaxel sensitivity in basal-like breast cancer. Cell Rep 26:3076–3086. https://doi.org/10.1016/j.celrep.2019.02.054.
38. Hou P, Ma X, Zhang Q, Wu CJ, Liao W, Li J, Wang H, Zhao J, Zhou X, Guan C, Ackroyd J, Jiang S, Zhang J, Spring DJ, Wang YA, DePinho RA. 2019. USP21 deubiquitinase promotes pancreas cancer cell stemness via Wnt pathway activation. Genes Dev 33:1361–1366. https://doi.org/10.1101/gad.326314.119.
39. Li W, Cui K, Prochownik EV, Li Y. 2018. The deubiquitinase USP21 stabilizes MEK2 to promote tumor growth. Cell Death Dis 9:482. https://doi.org/10.1038/s41419-018-0523-z.
40. Zhang J, Chen C, Hou X, Gao Y, Lin F, Yang J, Gao Z, Pan L, Tao L, Wen C, Yao Z, Tsun A, Shi G, Li B. 2013. Identification of the E3 deubiquitinase ubiquitin-specific peptidase 21 (USP21) as a positive regulator of the transcription factor GATA3. J Biol Chem 288:9373–9382. https://doi.org/10.1074/jbc.M112.374744.
41. Khan A, Giri S, Wang Y, Chakraborty A, Ghosh AK, Anantharaman A, Aggarwal V, Sathyan KM, Ha T, Prasanth KV, Prasanth SG. 2015. BEND3 represses rDNA transcription by stabilizing a NoRC component via USP21 deubiquitinase. Proc Natl Acad Sci U S A 112:8338–8343. https://doi.org/10.1073/pnas.1424705112.
42. Sato K, Rajendra E, Ohta T. 2008. The UPS: a promising target for breast cancer treatment. BMC Biochem 9(Suppl 1):S2. https://doi.org/10.1186/1471-2091-9-S1-S2.
43. Zhou J, Wang J, Chen C, Yuan H, Wen X, Sun H. 2018. USP7: target validation and drug discovery for cancer therapy. Med Chem 14:3–18. https://doi.org/10.2174/1573406413666171020115539.
44. Wang H, Liu Y, Huan C, Yang J, Li Z, Zheng B, Wang Y, Zhang W. 2020. NF-kappaB-interacting long noncoding RNA regulates HIV-1 replication and latency by repressing NF-kappaB signaling. J Virol 94:e01057-20. https://doi.org/10.1128/JVI.01057-20.
45. Wei W, Guo H, Gao Q, Markham R, Yu XF. 2014. Variation of two primate lineage-specific residues in human SAMHD1 confers resistance to N terminus-targeted SIV Vpx proteins. J Virol 88:583–591. https://doi.org/10.1128/JVI.02866-13.
46. Lv M, Zhang B, Shi Y, Han Z, Zhang Y, Zhou Y, Zhang W, Niu J, Yu XF. 2015. Identification of BST-2/tetherin-induced hepatitis B virus restriction and hepatocyte-specific BST-2 inactivation. Sci Rep 5:11736. https://doi.org/10.1038/srep11736.
47. Wang H, Guo H, Su J, Rui Y, Zheng W, Gao W, Zhang W, Li Z, Liu G, Markham RB, Wei W, Yu XF. 2017. Inhibition of Vpx-mediated SAMHD1 and Vpr-mediated host helicase transcription factor degradation by selective disruption of viral CRL4 (DCAF1) E3 ubiquitin ligase assembly. J Virol 91:e00225-17. https://doi.org/10.1128/JVI.00225-17.